Spinor Field Dark Energy in FLRW Space-time: Theory and Observation

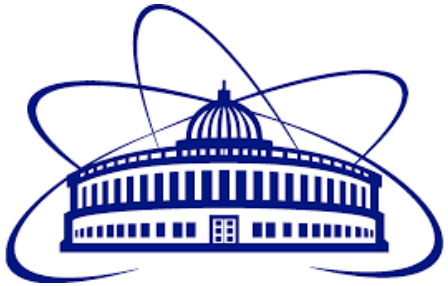

Bijan Saha

Laboratory of Information Technologies
JINR, Dubna, Russia



Dr. Mahendra Goray

Assistant Professor
Department of Physics, S.P. College
S.K.M. University, Dumka, India

MMCP 2026, JINR, Dubna 22-26 June, 2026

Outline

1. Introduction
2. Theoretical Model
3. Methodology
4. Results
5. Conclusion
6. Publications

Introduction : Aim and scope 3/37

In present-day cosmology, numerous theoretical models have been studied to account for the universe's accelerated expansion. Observational evidence from the Type Ia supernova (SNIa), Cosmic Microwave Background (CMB), Baryon Acoustic Oscillations (BAO), Surveys for growth of Large-Scale Structure (LSS), etc. has confirmed the acceleration of our universe. Even two and a half decades after discovering the accelerated universe, the reason behind it is still a mystery. However, it has been considered that an exotic component with negative pressure is responsible for the acceleration. Namely, it is called dark energy (DE); presently, it contains around two-thirds of the energy density of the universe.

Introduction: Aim and scope 4/37

In this work, we will further analyze the cosmological data sets under the framework of the spherically symmetric FLRW model filled with a spinor field. The spinor field nonlinearity generates different kinds of DE such as quintessence, generalized Chaplygin gas and modified Chaplygin gas. We parameterize the Hubble parameter $H(z)$, EoS, and all other cosmological parameters directly related to the spinor field DE model. To constrain the model parameter, we used the Markov Chain Monte Carlo (MCMC) statistical method in a Python 3.0 environment. The MCMC technique has been performed with the help of SNIa, Cosmic Chronometers (CC), and BAO data sets. More specifically, we combined supernova(binned) data, Observational Hubble Data (OHD), and Sloan Digital Sky Survey (SDSS) data sets, besides we simulated the full Pantheon data set only. Also, we compare our results with the Λ Cold Dark Matter (ΛCDM) model for the evolution of $H(z)$.

Basic equations: Spinor field Lagrangian 5/37

The spinor field Lagrangian we consider in the form

$$L_{\rm sp} = \frac{\imath}{2}\left[\bar{\psi}\gamma^{\mu}\nabla_{\mu}\psi - \nabla_{\mu}\bar{\psi}\gamma^{\mu}\psi\right] - m_{\rm sp}\bar{\psi}\psi - \lambda_0 F, \tag{1}$$

where the nonlinear term F describes the self-interaction of a spinor field and can be presented as some arbitrary functions of invariants K that take one of the following values $\{I,\ J,\ I+J,\ I-J\}$ generated from the real bilinear forms of a spinor field. We also consider the case $\psi = \psi(t)$ so that $I = S^2 = (\bar{\psi}\psi)^2$, & $J = P^2 = (\imath\bar{\psi}\gamma^5\psi)^2$. Here λ_0 is the self coupling constant.

Basic equations: FLRW model 6/37

The isotropic and homogeneous cosmological model proposed by Friedmann, Lemaitre, Robertson, and Walker independently are the most popular and thought to be realistic, one of the cosmologists. Let us consider the FLRW model in spherical coordinates in its standard form

$$ds^2 = dt^2 - a^2(t)\left[\frac{dr^2}{1-kr^2} + r^2 d\vartheta^2 + r^2 \sin^2\vartheta d\phi^2\right], \qquad (2)$$

with k taking the values $+1$, 0 and -1 which corresponds to a closed, flat, and open universe, respectively. Though the value of k defines the type of geometry of space-time, in reality, it is defined by the contents that fill universe. As we see later, independent to the value of k the universe filled with dark energy is always open, whereas for perfect fluid the value of k really matters. In this case depending on the value of k we obtain close, flat or open universe.

Basic equations: Energy-momentum tensor 7/37

The non-trivial components of the energy-momentum tensor of the spinor field in this case read

$$T_0^0 = mS + \lambda F := \varepsilon, \tag{3a}$$

$$T_1^1 = T_2^2 = T_3^3 = -\lambda\left(2KF_K - F\right) := -p, \tag{3b}$$

$$T_3^1 = \frac{a\cos\vartheta}{4\sqrt{1-kr^2}}A^0, \tag{3c}$$

$$T_1^0 = \frac{\cot\vartheta}{4r\sqrt{1-kr^2}}A^3, \tag{3d}$$

$$T_2^0 = -\frac{3}{4}\sqrt{1-kr^2}\,A^3, \tag{3e}$$

$$T_3^0 = \frac{3}{4}\sqrt{1-kr^2}\,\sin\vartheta A^2 - \frac{1}{2}\cos\vartheta A^1. \tag{3f}$$

Basic equations: Einstein equations 8/37

Since the FLRW metric contains only the diagonal components of the Einstein tensor, by setting the corresponding components of the stress-energy tensor to zero, we find

$$A^0 = 0, \quad A^3 = 0, \quad A^1 = \frac{3}{2}\sqrt{1 - kr^2}\,\tan\theta A^2. \tag{4}$$

The Einstein field equation

$$G^\mu_\nu = \kappa T^\mu_\nu, \tag{5}$$

reduce to

$$2\frac{\ddot{a}}{a} + \left(\frac{\dot{a}^2}{a^2} + \frac{k}{a^2}\right) = -8\pi G\, p, \tag{6a}$$

$$3\left(\frac{\dot{a}^2}{a^2} + \frac{k}{a^2}\right) = 8\pi G\, \varepsilon. \tag{6b}$$

Basic equations: Einstein equations 9/37

Introducing Hubble parameter H we rewrite foregoing system as

$$\dot{a} = Ha, \tag{7a}$$

$$\dot{H} = -H^2 - \frac{\kappa}{6}(\varepsilon + 3p). \tag{7b}$$

We solve this system numerically. In doing so, we have to provide a concrete form of spinor field nonlinearity as both energy density and pressure is given by the spinor field. Moreover, thanks to spinor field equations, equation (9) is fulfilled automatically. We just recall that the spinor field invariant can be given by

$$K = K_0/a^6, \tag{8}$$

which holds for any $K = \{I,\ J,\ I \pm J\}$ in a massless case, while for $K = I = S^2$ it holds for massive case as well.

Basic equations: Einstein equations 10/37

It should be noted that the Bianchi identity $G^{\nu}_{\mu;\nu} = 0$, which in this case is equivalent to $T^{\nu}_{\mu;\nu} = 0$ takes the form

$$\dot{\varepsilon} = -3H(\varepsilon + p), \tag{9}$$

and thanks to spinor field equations fulfills identically. Hence, it does not give any information about energy density and pressure. But we giving the equation of state $p = f(\varepsilon)$ we can find them. Here we consider quintessence, generalized Chaplygin gas and modified Chaplygin gas given by the following EoS respectively:

$$p = W\varepsilon, \quad W = \text{const.}, \tag{10a}$$

$$p = -A/\varepsilon^{\gamma}, \quad A > 0,\ 0 \leq \gamma \leq 1, \tag{10b}$$

$$p = W\varepsilon - A/\varepsilon^{\gamma}, \quad A > 0,\ 0 \leq \gamma \leq 1,\ W = \text{const.} \tag{10c}$$

Basic equations: Deceleration parameter and State finder 11/37

We also define two important parameters that we plot later. One of them is the deceleration parameter, which shows us whether the universe is expanding with acceleration.

$$q = -\frac{\ddot{a}}{aH^2} = -\left(\frac{\dot{H}}{H^2} + 1\right). \tag{11}$$

The state finder is a dimensionless cosmological diagnostic pairs constructed from scale factor and its derivatives only

$$r = \frac{\dddot{a}}{aH^3}, \quad s = \frac{r-1}{3(q-1/2)}. \tag{12}$$

Red Shift

In order to compare the results obtained theoretically it is better to rewrite the system (10) in terms of red-shift defined by

$$z = \frac{\lambda_o - \lambda_e}{\lambda_e}, \tag{13}$$

where λ_e and λ_o are the wave-lengths of emitted and detected light, respectively. It can be written in terms of scale factor

$$z + 1 = \frac{a_0}{a}, \tag{14}$$

where a_0 is the scale factor at present and can be taken to be unity. Beside this we also introduce luminosity distance

$$\dot{D}_L = c, \tag{15}$$

with c being the speed of light and can be taken unity.

Red Shift

Further we rewrite (7b) and (15) in terms of red-shift:

$$\frac{\partial H}{\partial z} = \frac{1}{(z+1)}\left[H + \frac{\kappa}{6H}(\varepsilon + 3p)\right], \tag{16a}$$

$$\frac{\partial D_L}{\partial z} = -\frac{1}{(z+1)H}. \tag{16b}$$

Further given the energy density ε and pressure p in term of spinor field nonlinearity we find theoretical values of for Hubble parameter and distance which is inverse proportional to luminosity.

Dark Energy Models 14/37

The spinor field nonlinearity corresponding to quintessence, generalized Chaplygin gas and modified Chaplygin gas are

$$F(K) = \lambda_1 K_0^{(1+W)/2}(1+z)^{3(1+W)} - m_{\rm sp}\sqrt{K_0}(1+z)^3, \tag{17a}$$

$$F(K) = \left(A + \lambda_1 K_0^{(1+\alpha)/2}(1+z)^{3(1+\alpha)}\right)^{1/(1+\alpha)}, \tag{17b}$$

$$F(K) = \left[\frac{A}{1+W} + \lambda_1 K_0^{(1+\alpha)(1+W)/2}(1+z)^{3(1+\alpha)(1+W)}\right]^{1/(1+\alpha)}. \tag{17c}$$

We consider massless spinor field. The constants λ_1 and K_0 can be taken to be unity. We have three parameters W, A and α those define the type of dark energy. We compare our theoretical results with Λ-CMD model to define these parameters to dins best fit results.

Data and Fitting 15/37

- **Cosmic Chronometers (CC)**: 43 measurements of the Hubble parameter $H(z)$, obtained via the differential age method, spanning the redshift interval $z \in [0.070, 2.36]$.
- **Sloan Digital Sky Survey (SDSS)**: 48 $H(z)$ data points extracted from BAO peak positions in galaxy clustering surveys, covering $z \in [0.0, 2.5]$.
- **Binned Pantheon Type Ia Supernovae (SNb)**: we use 40 binned distance modulus $\mu(z)$ data from the Pantheon compilation, distributed across $z \in [0.014, 1.612]$.
- **Baryon Acoustic Oscillation (BAO)**: 2 low-redshift BAO measurements, (**i**.) **6dF Galaxy Survey** at $z = 0.106$, given as $r_s/D_V(0.106) = 0.336 \pm 0.015$, (**ii.**) **SDSS-MGS survey** at $z = 0.15$, given as $D_V(0.15)/r_s = 4.466 \pm 0.168$.

Data and Fitting 16/37

In case of Binned Pantheon Type Ia Supernovae (SNb) the observed quantity is the distance modulus $\mu(z)$

$$\mu(z) = 5\log_{10}\left(\frac{D_L(z)}{\text{Mpc}}\right) + 25, \tag{18}$$

where the luminosity distance $D_L(z)$ is defined in terms of the comoving distance $D_C(z)$ as

$$D_L(z) = (1+z)D_C(z), \quad D_C(z) = c\int_0^z \frac{dz'}{H(z')}. \tag{19}$$

Here, c is the speed of light in km/s, and $H(z)$ is the Hubble parameter. The total uncertainty in the observed distance modulus includes both the statistical uncertainty from measurements and an intrinsic scatter σ_{int}, such that the total error is

$$\sigma_{\mu,\text{tot}} = \sqrt{\sigma_\mu^2 + \sigma_{\text{int}}^2}. \tag{20}$$

We adopt a constant $\sigma_{\text{int}} = 0.13$ mag, consistent with recent literature.

Data and Fitting 17/37

In case of Baryon Acoustic Oscillation (BAO) we define the volume-averaged distance as

$$D_V(z) = \left[(1+z)^2 D_A^2(z) \cdot \frac{cz}{H(z)}\right]^{1/3} \tag{21}$$

where $D_V(z)$ is the angular diameter distance computed from the comoving distance. Although the DESI DR1 BAO dataset provides substantially more precise measurements across multiple redshifts, we have not included it here because its proper use requires the incorporation of the full covariance matrix between $D_M(z)/r_d$ and $H(z)r_d/c$. Our current likelihood pipeline is optimized for the legacy BAO data, and an extension to include the DESI dataset is planned for a forthcoming work.
Numerical experiment was carried out using python Jupiter Notebook. We used following ranges $H \in (50, 90)$ km/mega parsec and $-2 < W < 0$.

Data and Fitting 18/37

- **Likelihood function:** χ^2 from H(z) and SN data. The total chi-square function employed in the likelihood analysis is defined as

$$\chi^2_{\text{total}} = \chi^2_{\text{OHD}} + \chi^2_{\text{SDSS}} + \chi^2_{\text{SNb}} + \chi^2_{\text{BAO}}, \tag{22}$$

where χ^2_{OHD}, χ^2_{SDSS}, χ^2_{SNb}, and χ^2_{BAO} represent the individual contributions from the cosmic chronometer (CC), Sloan Digital Sky Survey (SDSS), Pantheon binned Type Ia Supernovae (SNb), and baryon acoustic oscillation (BAO) datasets, respectively. Each chi-square term is computed via

$$\chi^2 = \sum_{i=1}^{N} \left(\frac{O_i - T_i}{\sigma_i} \right)^2, \tag{23}$$

where O_i denotes the observed value and T_i is the corresponding theoretical prediction of Hubble parameter H from the model, σ_i is the measurement uncertainty, and N is the total number of data points in the respective dataset.

MCMC Corner Plot (GCG model)

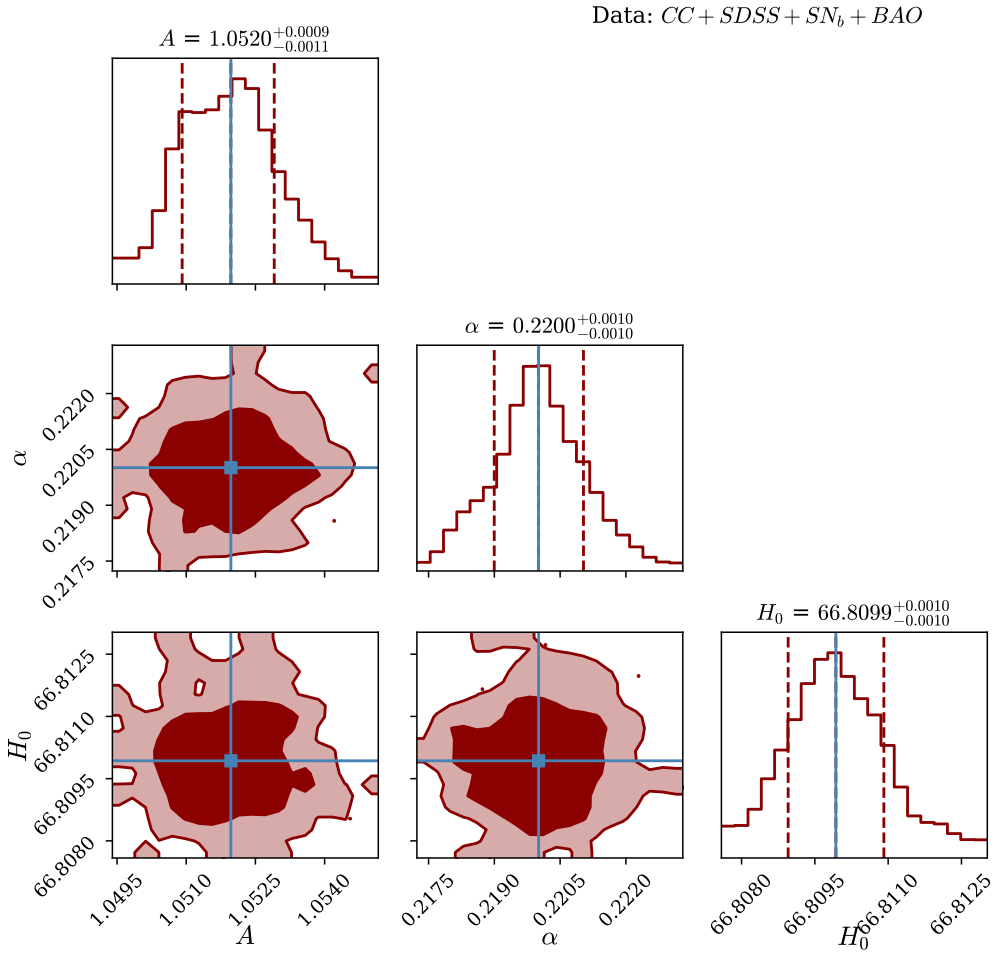

Figure: Posterior distributions of model parameters of GCG model.

MCMC Corner Plot (Quintessence model) 20/37

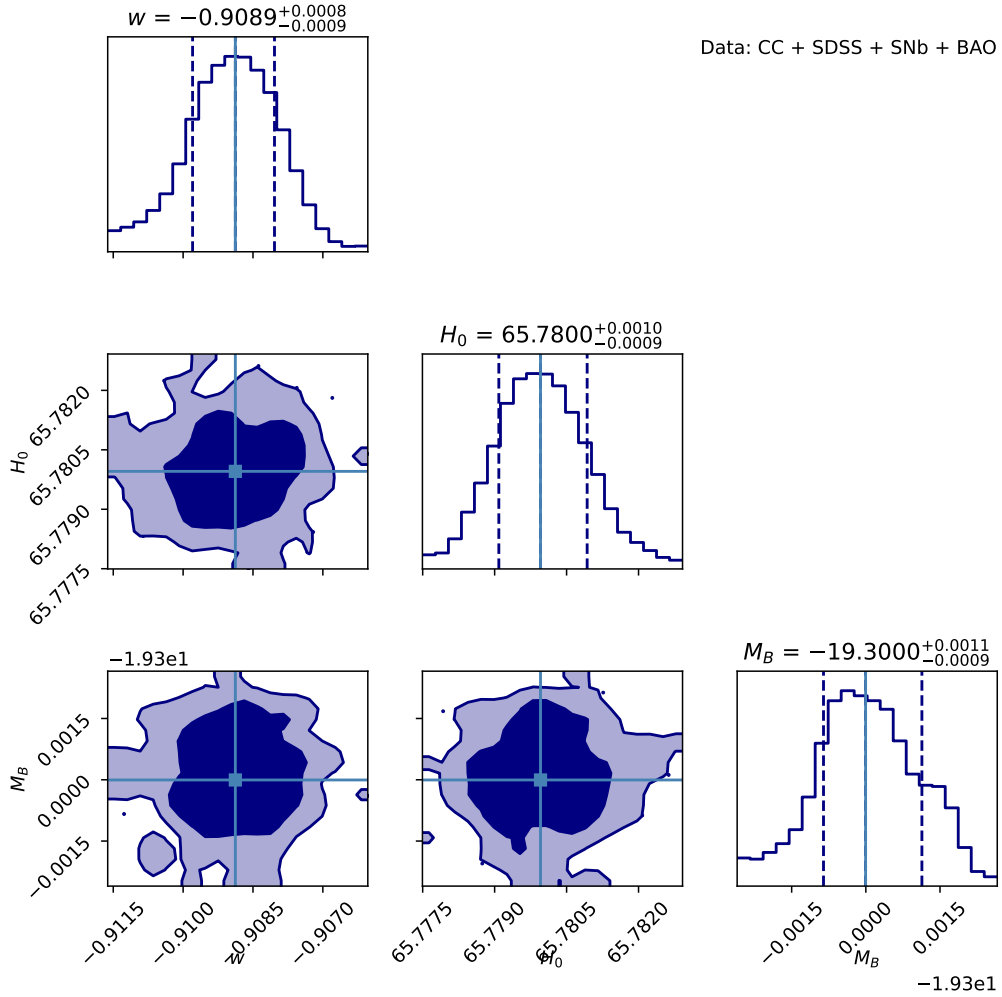

Figure: Posterior distributions of model parameters of the Quintessence model.

MCMC Corner Plot (MCG model) 21/37

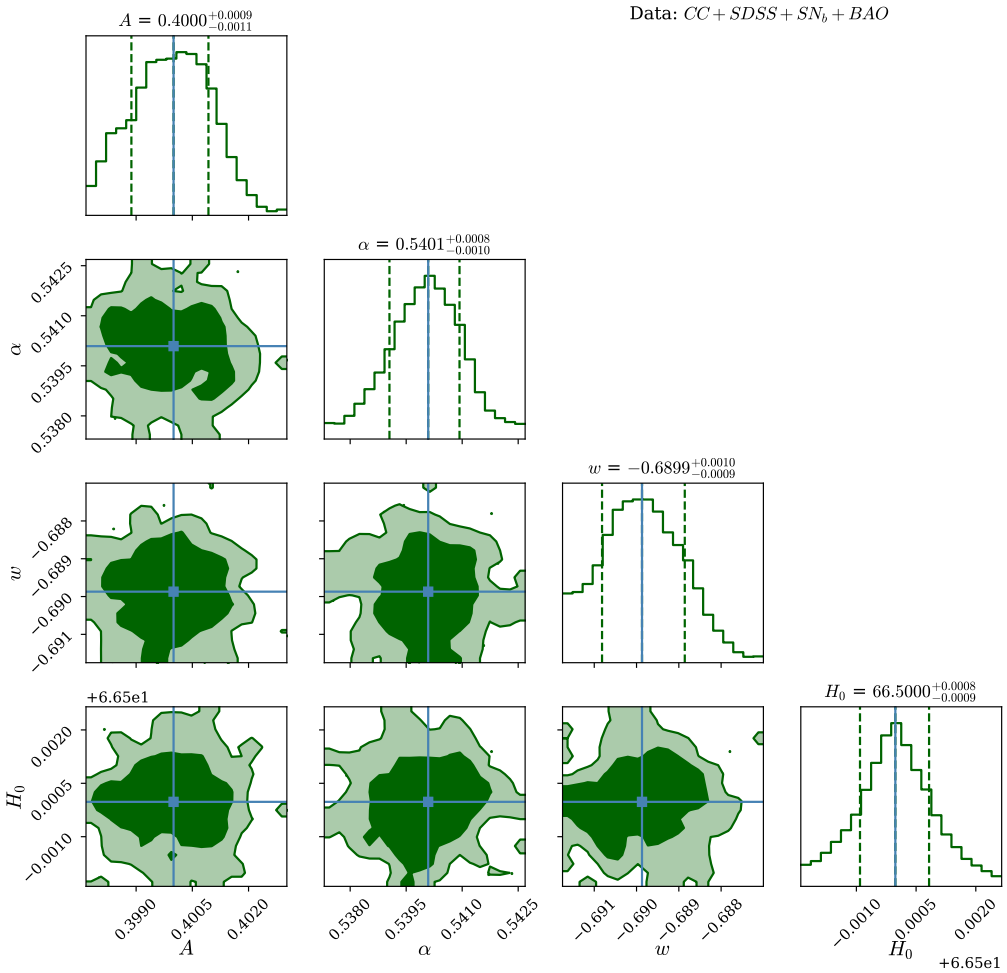

Figure: Posterior distributions of model parameters of MCG model.

MCMC Corner Plot (ΛCDM model) 22/37

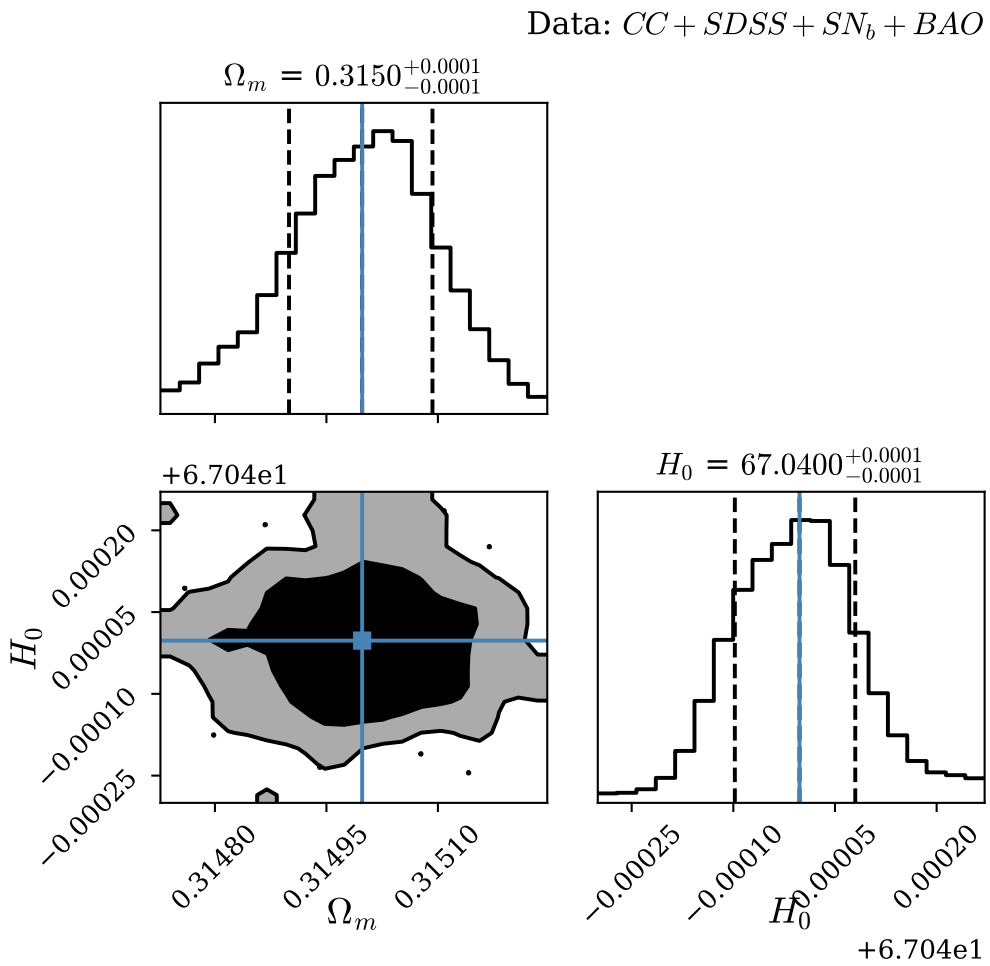

Figure: Posterior distributions of model parameters of ΛCDM model.

MCMC Results

Table: Best-fit cosmological parameters for different dark energy models using the combined dataset (CC + SDSS + SNb + BAO).

Model	A	α	w	Ω_m	H_0 (km s^{-1} Mpc^{-1})
GCG	1.05191	0.22007	–	–	66.829
Quintessence	–	–	−0.909	–	65.780
MCG	0.39998	0.53990	−0.690	–	66.500
ΛCDM	–	–	−1.000	0.3150	66.560

Table: Statistical comparison of different cosmological models using the combined dataset (OHD + SDSS + SN$_b$ + BAO). The last two columns show the differences ΔAIC and ΔBIC relative to the ΛCDM model.

Model	Parameters	$\chi^2_{\rm Total}$	AIC	BIC	χ^2_ν	ΔAIC	ΔBIC
GCG	3	139.773	145.773	154.329	1.118	5.411	8.323
Quintessence	2	140.286	144.286	149.990	1.113	3.924	3.924
MCG	4	132.824	140.824	152.232	1.071	0.462	6.166
ΛCDM	2	136.362	140.362	146.066	1.082	**0.000**	**0.000**

Equation of State $w(z)$

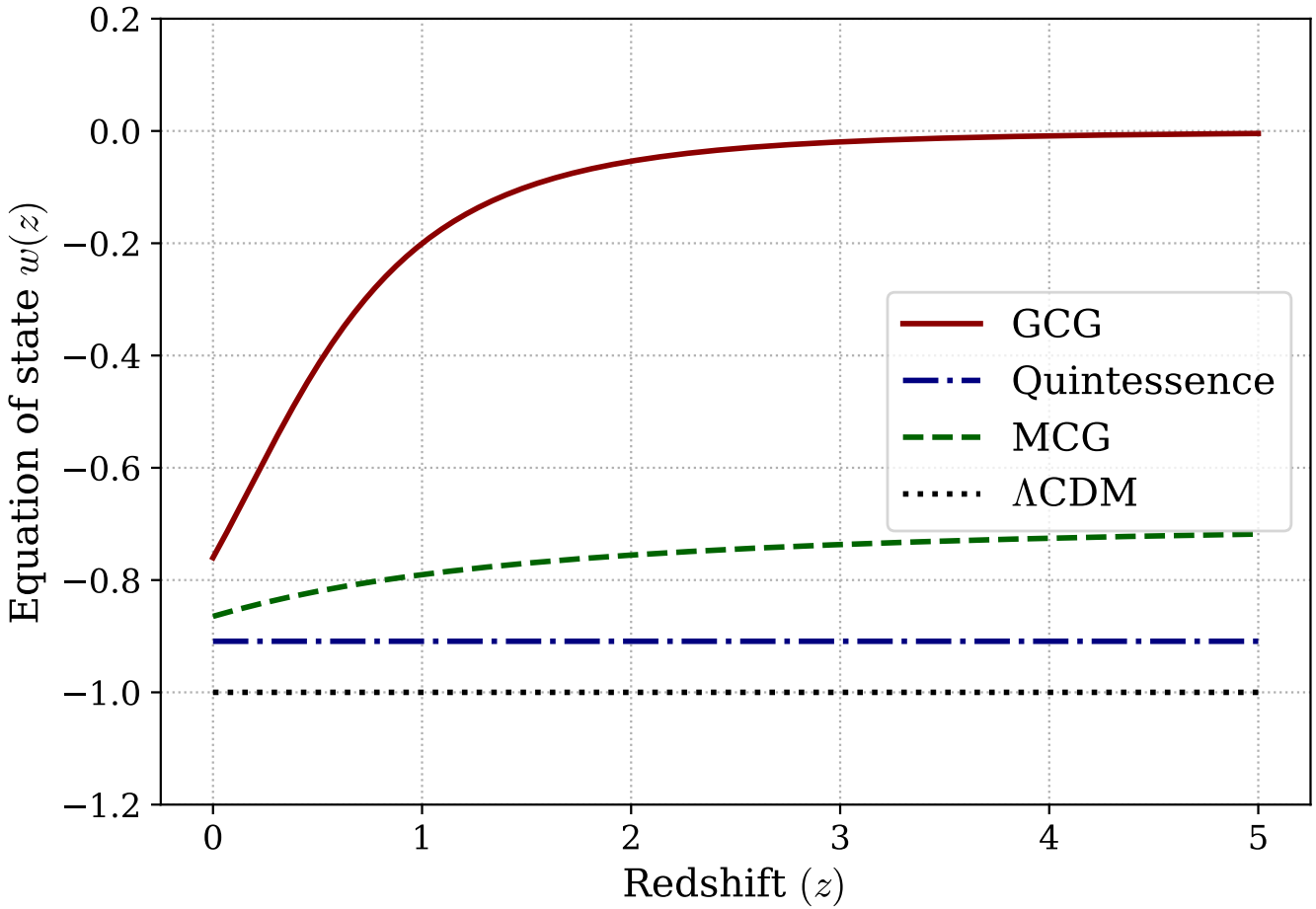

Figure: Effective equation of state of spinor field dark energy.

Deceleration Parameter $q(z)$

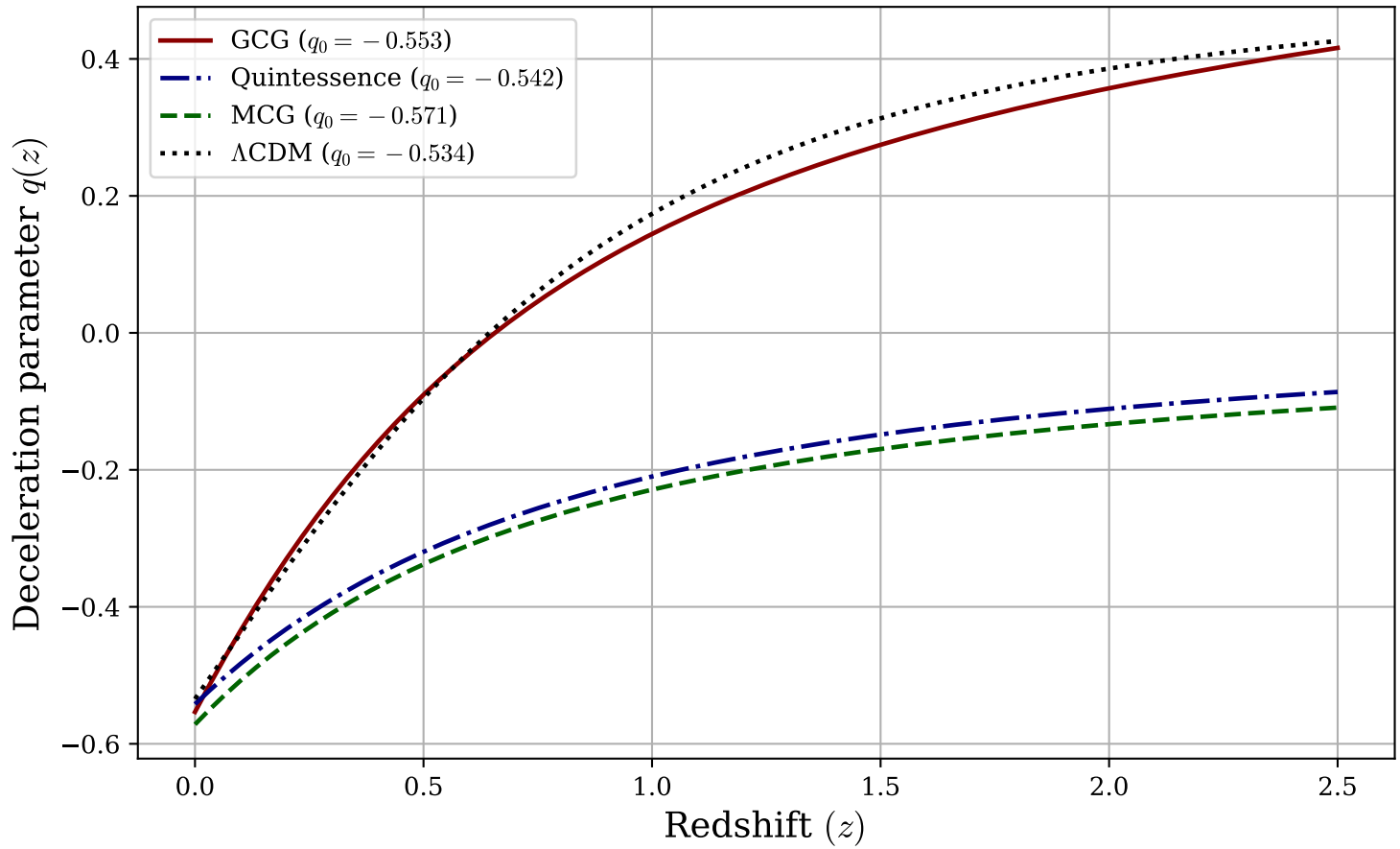

Figure: Deceleration parameter as a function of redshift.

Statefinder (r, s): Evolution

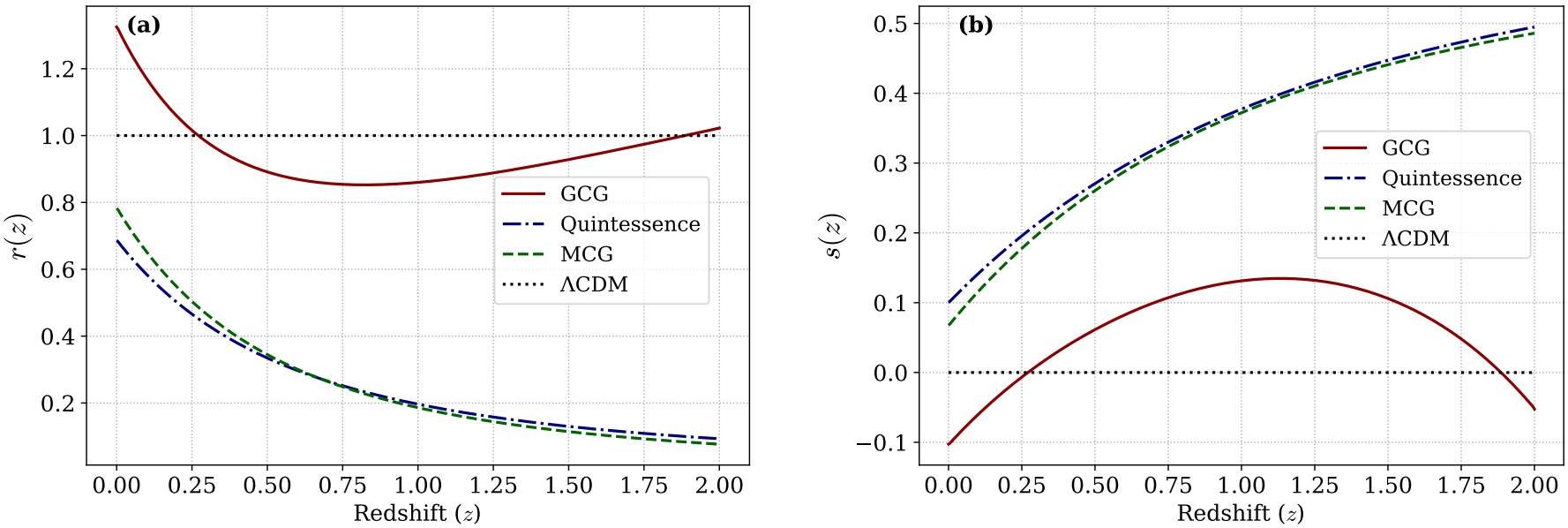

Figure: Statefinder parameters $r(z)$ and $s(z)$.

Statefinder (r, s): Trajectories

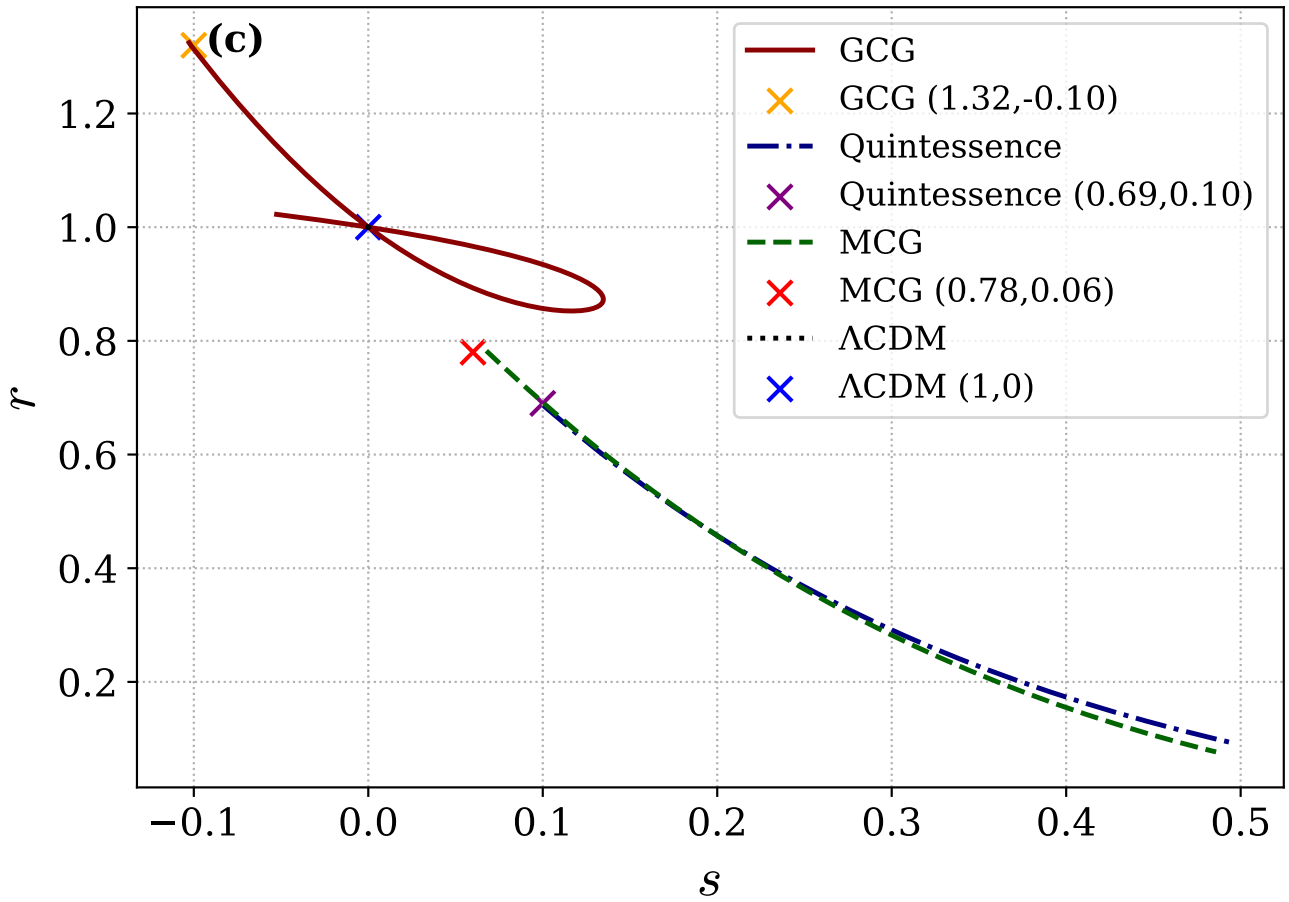

Figure: $r - s$ trajectories for different models.

Present-day values of the $w_0, q_0, (r_0, s_0)$ 28/37

Table: Present-day values of the deceleration parameter q_0, statefinder pair (r_0, s_0), and equation-of-state parameter w_0 for the spinor GCG, spinor MCG, spinor quintessence, and ΛCDM models. The statistically preferred model is highlighted in bold.

Model	w_0	q_0	r_0	s_0
GCG	-0.760	-0.5534	1.3246	-0.1027
Quintessence	-0.909	-0.5420	0.6863	0.1004
MCG	$\mathbf{-0.864}$	$\mathbf{-0.5719}$	**0.7825**	**0.0676**
ΛCDM	-1.000	-0.5545	1.0003	-0.0001

Hubble Parameter $H(z)$

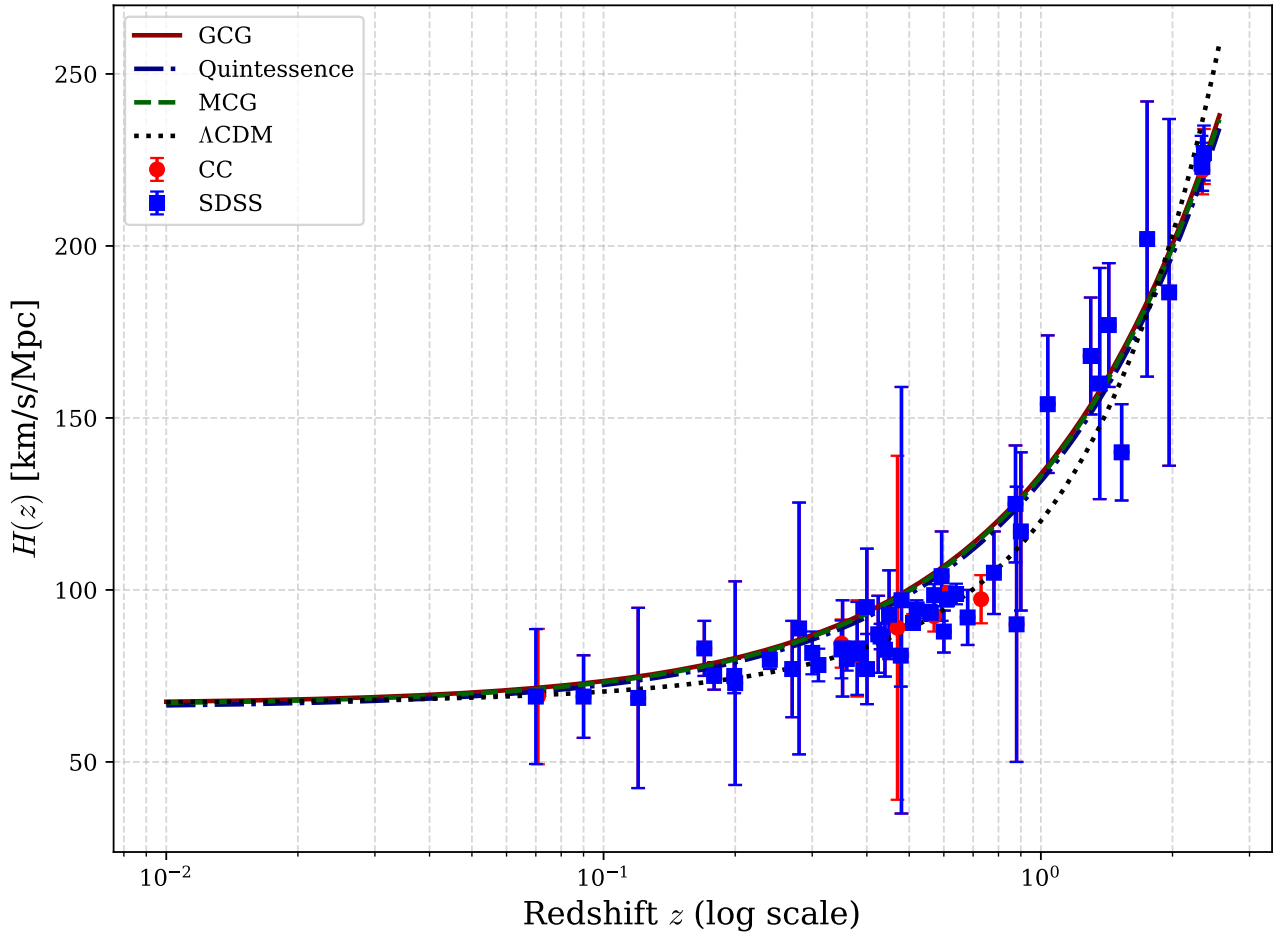

Figure: Hubble parameter vs redshift.

Distance Modulus $\mu(z)$

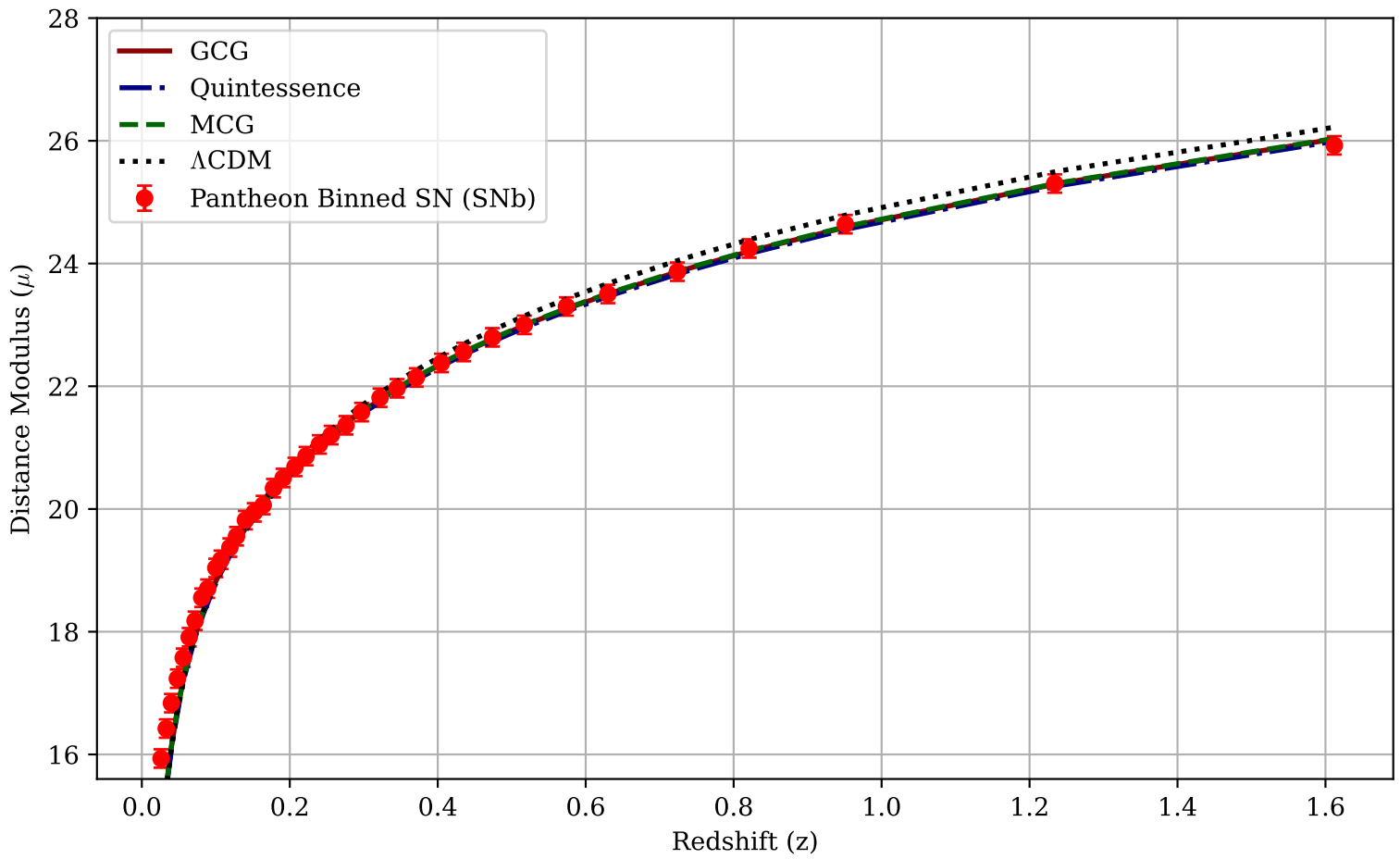

Figure: Distance Modulus vs redshift, from Type Ia SN data.

Residual: $\mu_{obs} - \mu_{model}$

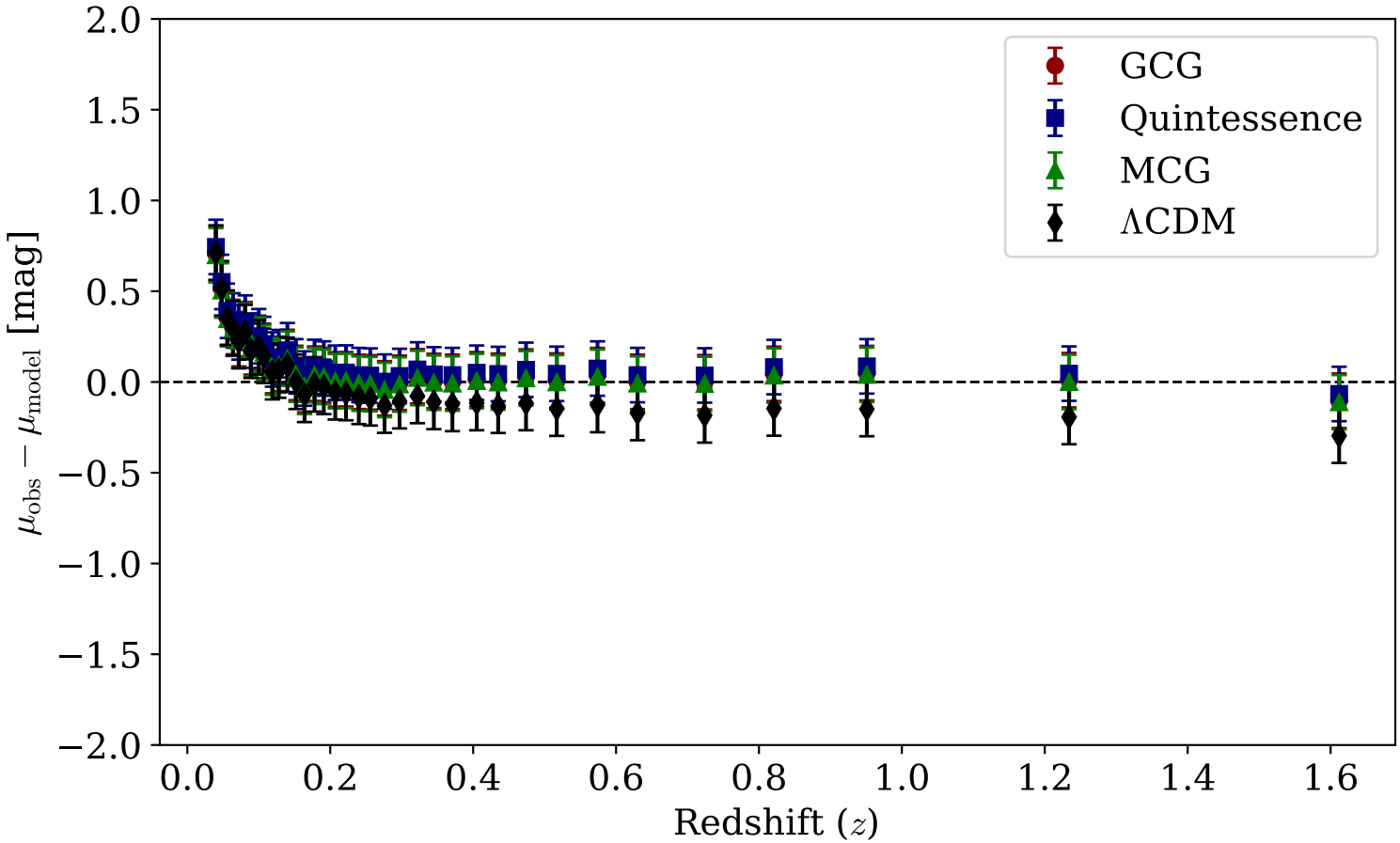

Figure: Residuals of Distance Modulus

Conclusion 32/37

- Spinor field provides a viable model for dark energy.
- Fits observational H(z) and SN data well.
- Future work: Include CMB constraints, explore non-minimal couplings.

All these works need more powerful computational facilities. Unfortunately, my coauthor Dr. Goray lacks the facilities which we have in LIT. Hope, some day he can visit LIT and make full use of our resources.

Publications 33/37

- B. Saha, *"Nonlinear spinor field in Bianchi type-I cosmology: inflation, isotropization, and late time acceleration"* *PRD* **74**, 124030 (2006) DOI: 10.1103/PhysRevD.74.124030
- B. Saha, *"Spinor field nonlinearity and space-time geometry"* *Physics of Particles and Nuclei*, **49**(2), 146 - 212 (2018) . DOI: 10.1134/S1063779618020065
- B. Saha, *"Spinor field in FLRW cosmology: spherically symmetric case"* *Journal of Experimental and Theoretical Physics*, **167** (1), 49 - 58 (2025) DOI: 10.31857/S0044451025010043

Publications 34/37

- Mahendra Goray, B. Saha, *"Observational Constraints on a Spinor Field Generalized Chaplygin Gas Model in a Spherically Symmetric FLRW Spacetime"* *EPJC*, **85**(10), 1146 (2025). DOI: 10.1140/epjc/s10052-025-14895-3
- Mahendra Goray, B. Saha, *"Observational constraints on a nonlinear spinor field quintessence model in an FLRW universe"* *EPJC*, **86**(1), 19 (2026). DOI: 10.1140/epjc/s10052-025-15230-6
- Mahendra Goray, B. Saha, *"Spinor-Field Realization of Modified Chaplygin Gas Dark Energy in FLRW Cosmology and Observational Constraints"* *Nuclear Phys. B*, **1027**, 117468 (2026). https://doi.org/10.1016/j.nuclphysb.2026.117468

References

- N. Aghanim et al. (Planck Collaboration), Planck 2018 results. VI. Cosmological parameters. Astron. Astrophys. **641**, A6 (2020).
- S. Alam et al.(eBOSS), Completed sdss-IV extended baryon oscillation spectroscopic survey: cosmological implications from two decades of spectroscopic surveys at the apache point observatory. Phys. Rev. D **103**, 083533 (2021).
- DESI Collaboration, DESI 2024 results: First cosmology from baryon acoustic oscillations. Astrophys. J. Lett. **973**, L14 (2024).

References

- I. Imdiker, M.P. Dabrowski, and V. Salzano, Generalized nonextensive entropy holographic dark energy models verified by cosmological data. Eur. Phys. J. C **85**, 775 (2025).
- S. Aiola et al. (ACT Collaboration), The Atacama Cosmology Telescope: DR4 maps and cosmological parameters. JCAP **12**, 047 (2020).
- A.L. Posta et al., Constraints on prerecombination early dark energy from SPT-3G public data. Phys. Rev. D **105**, 083519 (2022).

Thank You!